

# Shifts and widths of p-wave confinement induced resonances in atomic waveguides

Shahpoor Saeidian,<sup>1,\*</sup> Vladimir S. Melezhik,<sup>2,3,†</sup> and Peter Schmelcher<sup>4,5,‡</sup>

<sup>1</sup>*Optics and Photonics Research Center, Department of Physics,  
Institute for Advanced Studies in Basic Sciences (IASBS), Gava Zang, Zanjan 45137-66731, Iran*

<sup>2</sup>*Bogoliubov Laboratory of Theoretical Physics, Joint Institute for Nuclear Research,  
Dubna, Moscow Region 141980, Russian Federation*

<sup>3</sup>*Department of Theoretical Physics, Dubna International University for Nature,  
Society and Man, Dubna, Moscow Region 141980, Russian Federation*

<sup>4</sup>*Zentrum für Optische Quantentechnologien, Universität Hamburg,  
Luruper Chaussee 149, 22761 Hamburg, Germany*

<sup>5</sup>*The Hamburg Center for Ultrafast Imaging, Luruper Chaussee 149, 22761, Hamburg, Germany*  
(Dated: October 13, 2018)

We develop and analyze a theoretical model to study p-wave Feshbach resonances of identical fermions in atomic waveguides by extending the two-channel model of A.D. Lange et. al. [Phys. Rev. A 79, 013622 (2009)] and S. Saeidian et. al. [Phys. Rev. A 86, 062713 (2012)]. The experimentally known parameters of Feshbach resonances in free space are used as input of the model. We calculate the shifts and widths of p-wave magnetic Feshbach resonance of <sup>40</sup>K atoms emerging in harmonic waveguides as p-wave confinement induced resonance (CIR). Particularly, we show a possibility to control the width and shift of the p-wave confinement induced resonance by the trap frequency and the applied magnetic field which could be used in corresponding experiments. Our analysis also demonstrates the importance of the inclusion of the effective radius in the computational schemes for the description of the p-wave CIRs contrary to the case of s-wave CIRs where the influence of this term is negligible.

PACS numbers: 32.60.+i, 33.55.Be, 32.10.Dk, 33.80.Ps

## I. INTRODUCTION

The recent progress in ultracold atomic physics provides exceptional possibilities for studying low-dimensional quantum systems. The confining geometry of atomic traps can drastically alter their ultracold scattering behaviour near the so-called confinement induced resonances (CIRs) [1]. Employing magnetic Feshbach resonances [2], one can control the interaction between the atoms and provide the conditions to experimentally observe the CIRs for identical bosons [3–6] and fermions [7–9], as well as distinguishable atoms [10]. CIRs have been extensively studied, e.g. in the context of bosonic s- [11–13] and d-wave [14] and dipolar [15, 16] scattering, fermionic p-wave scattering [12, 17], distinguishable atom scattering [12, 18–20] in single-channel as well as in multichannel (transversal excitation) regimes [13, 21, 22]. Beyond this coupled l-wave CIRs in cylindrically symmetric waveguides have been explored [23, 24].

In spite of the impressive progress concerning the experimental [6, 9, 10, 25] and theoretical [21, 26–28] investigations of CIRs the existing theoretical models need to be improved for a quantitative interpretation and guiding of the experiments. In the seminal work of Olshanii [1] and in subsequent works [11, 26, 27, 29, 30], the sim-

ple form of a pseudo-potential was used to model the interatomic interactions as compared to CIR investigations with more realistic interatomic potentials [11, 13, 14, 17–21, 28, 31]. However, all these approaches are of single-channel (internal) character, allowing one to explore only the main attribute of the Feshbach resonances in the 3D free space, i.e. the appearance of a singularity in the s-wave scattering length  $a_s \rightarrow \pm\infty$  when a molecular bound state with energy  $E_B$  crosses the atom-atom scattering threshold at energy  $E = 0$  in the entrance channel. However, other important parameters of the Feshbach resonance, such as the rotational and spin structure of the molecular bound state in the closed channel as well as the width  $\Delta$  of the resonance characterizing the coupling  $\Gamma$  of the molecular state with the entrance channel, were ignored. In our recent work [32] the single-channel scalar interatomic interaction was replaced by the four-channel tensorial potential modeling resonances of broad, narrow, and overlapping character for bosons, according to the two-channel parametrization suggested in [33]. This allowed us to calculate the shifts and widths of s-, d-, and g-wave magnetic Feshbach resonances of Cs atoms emerging in harmonic waveguides as CIRs.

In the present work our particular focus are p-wave collisions of identical fermions due to their anisotropic character. Confinement induced shifts and widths of the resonances in an atomic waveguide could be envisaged, similar to what has been studied for s-wave interactions [32]. The main goal of the present work is therefore to extend our model [32] to the fermionic case. We then calculate the shifts and widths of the Feshbach resonance for

\*saeidian@iasbs.ac.ir

†melezhik@theor.jinr.ru

‡peter.schmelcher@physnet.uni-hamburg.de

$^{40}\text{K}$  atoms in its hyperfine state  $|F = 9/2, m_F = -7/2\rangle$  for experimental conditions [8]. The parameters which can be obtained from the experiments on magnetic Feshbach resonances in free space [34, 35], namely, the spin characteristics, the background scattering volume  $V_{bg}$ , the resonant energies  $E_c$  (or the corresponding resonant value of the strength  $B_c$  of the external magnetic field), and the width of the resonance  $\Delta$  ( $\Gamma$ ) are used as input parameters of our model.

## II. FESHBACH RESONANCE MODEL IN FREE SPACE

Let us first discuss an extension of our model [32], developed for resonant s-wave scattering, to the case of p-wave Feshbach resonances in 3D free space which can be observed in a single-component Fermi gas. Due to the Pauli exclusion principle the two-body wave function must be antisymmetric, and therefore only odd partial waves  $l$  contribute to the fermionic scattering process in case of a symmetric spin configuration. In contrast to the s-wave Feshbach resonance, the atoms near a p-wave Feshbach resonance have to tunnel through a centrifugal barrier to couple to the bound molecular state. Therefore, the wave function of the continuum can be significantly influenced by the bound state in the closed channel only in a narrow range of the magnetic field. Another feature of the p-wave Feshbach resonances is a doublet structure which arises from the magnetic dipole-dipole interaction between the electronic spins of the atoms. This splits the Feshbach resonance into distinct resonances indicated by their partial-wave projection  $m_l = 0$  and  $|m_l| = 1$  along the quantization axis.

In this work we investigate collisions of two spin-polarized  $^{40}\text{K}$  atoms in the hyperfine state  $|F = 9/2, m_F = -7/2\rangle$ . One can write the joint state of the atom pair as  $|f_1 = 9/2, m_{f_1} = -7/2\rangle|f_2 = 9/2, m_{f_2} = -7/2\rangle|l = 1, m_l\rangle$  where  $m_l = 0, \pm 1$ . The dipole-dipole interaction between the valence electrons of the atom pairs can be written as

$$H_{ss} = -\alpha^2 \frac{3(\hat{\mathbf{r}} \cdot \hat{\mathbf{S}}_1)(\hat{\mathbf{r}} \cdot \hat{\mathbf{S}}_2) - (\hat{\mathbf{S}}_1 \cdot \hat{\mathbf{S}}_2)}{r^3}$$

where  $\alpha$  is the fine structure constant,  $\hat{\mathbf{S}}_i$  is the spin of the valence electron of  $i$ th atom,  $r$  is the interatomic separation, and  $\hat{\mathbf{r}}$  is the unit vector defining the direction of interatomic axis. It couples different partial wave components  $|l, m_l\rangle$  and  $|l', m'_l\rangle$  with  $l' = l \pm 2$  or  $l' = l \neq 0$  [34], and breaks the rotational invariance. The different components  $m_l$  contribute differently in the dipole-dipole interaction, which means that molecular bound states with different  $m_l$  possess different energies [34]. Consequently, the Feshbach resonances for different  $m_l$  values couple to distinct molecular bound states and thus have different magnetic-field dependence.

The difference in the pair collisions with the different  $m_l$  projections can be understood intuitively by consider-

ing the dipole-dipole interaction between the two atoms. The external magnetic field orients the spin of the valence electron of  $^{40}\text{K}$  in  $|F = 9/2, m_F = -7/2\rangle$  state. When two dipoles are aligned side-by-side (head-to-tail), they are in a repulsive (attractive) configuration, corresponding to  $(\hat{\mathbf{r}} \cdot \hat{\mathbf{S}}_i) = 0$  ( $(\hat{\mathbf{r}} \cdot \hat{\mathbf{S}}_i) = 1$ ).

The difference between the states  $m_l = 0$  and  $|m_l| = 1$  is illustrated in Fig.3 of ref.[34]. In the case the motion is in a plane containing the magnetic field the interaction alternates between attractive and repulsive as the dipoles change between head to tail attraction and side by side repulsion. On the other hand, for the case that the atoms move in the plane perpendicular to the magnetic field the dipoles are held in the side-by-side configuration, and the interaction is only repulsive. Due to this effect one expects that the dipole-dipole interaction lifts the degeneracy between the  $m_l = 0$  and  $|m_l| = 1$  collisional channels which leads to a splitting of the Feshbach resonances, with corresponding resonance for  $|m_l| = 1$  at a higher energy [34]. This doublet structure disappears with increasing temperature due to a broadening of the resonance.

For p-wave collisions the relevant parameter is the scattering volume,  $V_p$  which has been parameterized as [34]

$$k^3 \cot \delta_1(k, B) = -\frac{1}{V_p(B)} + \frac{k^2}{R(B)} \quad (1)$$

near the magnetic Feshbach resonance, where  $V_p$  and the effective range  $R$  were approximated as a quadratic function of the magnetic field  $B$

$$\frac{1}{V_p(B)} = c^{(0)} + c^{(1)}B + c^{(2)}B^2 \quad (2)$$

$$\frac{1}{R(B)} = d^{(0)} + d^{(1)}B + d^{(2)}B^2. \quad (3)$$

The coefficients  $c^{(i)}$  and  $d^{(i)}$  were obtained by fitting to the experimental data and are given in Table I of [35]. A simple formula for an energy-dependent scattering volume has been derived in the framework of multichannel quantum-defect theory (MQDT)

$$V_p(E, B) = V_{bg}(E) \left[ 1 - \frac{\Delta(1 + \frac{E^3}{E_{bg}^3})}{B - B_0 - \frac{E}{\delta\mu} + \frac{E^3}{E_{bg}^3}} \right], \quad (4)$$

where  $E_{bg} = \frac{\hbar^2}{2\mu a_{bg}^2}$  is the energy associated with the background scattering length  $a_{bg} = \lim_{E \rightarrow 0} [V_{bg}(E)]^{1/3}$  ( $\mu = m/2$  is the reduced mass). Except for the case  $a_{bg} \gg R_{vdW}$ ,  $E_{bg} \sim E_{vdW}$ , and therefore  $E \ll E_{vdW}$  (here  $R_{vdW} = 1/2(2\mu C_6/\hbar^2)^{1/4}$  is the van der Waals radius,  $C_6$  is the corresponding van der Waals coefficient and  $E_{vdW} = \hbar^2/2\mu R_{vdW}^2$ ), when one does not need to take into account the effective range expansion of  $V_{bg}(E)$ ,

$ m_l $	$B_0[G]$	$B^*[G]$	$\frac{\Gamma}{h}[MHz]$	$\Delta[G]$	$\frac{\delta\mu}{h}[\frac{kHz}{G}]$	$a_{bg}[a_0]$
0	198.85	178.508	0.5684	-20.342	93.093	-104.26
1	198.37	175.414	0.6950	-22.956	92.667	-99.539

TABLE I: The poles  $B_0$  and zeros  $B^*$  of the scattering volume  $V_p(B)$ , the coupling strength  $\Gamma$ , the resonance width  $\Delta$ , the magnetic moment difference  $\delta\mu$  and the background scattering length  $a_{bg}$  for a p-wave Feshbach resonance between two  $^{40}\text{K}$  atoms in the hyperfine state  $|F = 9/2, m_F = -7/2\rangle$  for two relative angular momentum projections  $m_l$  along the axis of the magnetic field.

Eq.(4) can be simplified to

$$V_p(E, B) = V_{bg} \left[ 1 - \frac{\Delta}{B - B_0 - \frac{E}{\delta\mu}} \right] \quad (5)$$

Fitting the expansion (1) to this formula, one obtains the resonance parameters listed in Table I [35].

Using MQDT in the two channel case, the following formula for the phase shift in the open channel

$$\delta(E, l) = \delta_{bg}(E, l) - \arctan \left( \frac{\frac{\Gamma}{2} C^{-2}(E, l)}{E - E_c + \frac{\Gamma}{2} \tan \lambda(E, l)} \right) \quad (6)$$

was obtained in ref.[35]. The first term  $\delta_{bg}(E, l)$  is the phase shift resulting from the scattering in the open channel only, i.e. the background phase shift. The second term describes the resonant contribution originating from a bound state in the closed channel with the energy  $E_c$  located close to the threshold of the open channel.  $C^{-2}(E)$  and  $\tan \lambda(E)$  are MQDT functions. The width of the resonance  $\Gamma$  is multiplied by  $C^{-2}(E)$  which accounts for a proper threshold behaviour as  $k \rightarrow 0$ .

We assume that the bound state can be linearly tuned by a magnetic Zeeman shift, i.e.  $E_c(B) = \delta\mu(B - B_c)$ , where  $\delta\mu$  is the difference of the magnetic moments of the open and closed channels, and  $B_c$  is the crossing field value of the bound state. In the case of a power law interaction potential  $r^{-s}$  the phase shift and MQDT function exhibit the following Wigner threshold behavior as  $E \rightarrow 0$  [35]

$$\delta_{bg}(E) \longrightarrow A_l k^{2l+1} \quad (7)$$

for  $2l + 1 \leq s - 2$  and

$$C^{-2}(E) \longrightarrow B_l k^{2l+1} \quad (8)$$

and

$$\tan \lambda(E) \longrightarrow \tan \lambda(0) \quad (9)$$

for all  $l$ . For van der Waals forces the higher order terms in  $k$  can be neglected in case  $E \lesssim E_{vdW}$ . For alkali atoms  $E_{vdW}$  ranges from 0.1mK to 30mK [36]. Hence, in the ultracold regime ( $E \lesssim 1\mu\text{K}$ ), one can safely use

the approximation (7)-(9). The width  $\Delta$  of the magnetic Feshbach resonance reads

$$\lim_{E \rightarrow 0} \frac{\Gamma}{2} \frac{C^{-2}(E)}{\tan \delta_{bg}(E)} = -\delta\mu\Delta \quad (10)$$

and the resonance position  $B_0$ , that is shifted from  $B_c$  due to the coupling between the open and closed channels take on the following appearance

$$B_0 = B_c + \frac{\Gamma}{2\delta\mu} \lim_{E \rightarrow 0} \tan \lambda(E). \quad (11)$$

Further, using the above parametrization, we extend the scheme suggested in ref.[33] to describe the magnetic Feshbach resonances of the p-wave scattering in an ultracold  $^{40}\text{K}$  gas. The two-body problem in free space permits the separation of the center-of-mass and relative motion yielding the following Hamiltonian for the relative atomic motion

$$\hat{H}(r, \theta) = \left[ -\frac{\hbar^2}{2\mu} \nabla^2 \right] \hat{I} + \hat{V}(r) \quad (12)$$

Here  $\hat{V}(r)$  is the two-channel interatomic potential and  $\hat{I}$  is the unit matrix and  $r$  is the relative radial coordinate. Let us suppose that initially the spin-polarized atoms are prepared in the entrance channel  $|e\rangle$  and the “closed channels”  $|c\rangle$  supports molecular bound states at  $B_0$ . The quantum state of an atomic pair with energy  $E$  is then described as  $|\psi\rangle = \psi_c(\mathbf{r})|c\rangle + \psi_e(\mathbf{r})|e\rangle$  satisfying the Schrödinger equation with the Hamiltonian (12). A two-channel square-well potential

$$\hat{V} = \begin{pmatrix} -V_c & \hbar\Omega \\ \hbar\Omega & -V_e \end{pmatrix} \quad (\text{if } r < \bar{a}) \quad (13)$$

$$= \begin{pmatrix} \infty & 0 \\ 0 & 0 \end{pmatrix} \quad (\text{if } r > \bar{a})$$

is employed to describe the colliding atoms in the “entrance channel”  $|e\rangle$  and the weakly-bound molecule in the “closed channel”  $|c\rangle$  near a Feshbach resonance. The coupling constant  $\hbar\Omega$  induces Feshbach couplings between the channels. For  $r < \bar{a}$ , we assume that the attractive potential supports multiple molecular states - that is  $V_e, V_c \gg E_{vdW} = \hbar^2/2\mu R_{vdW}^2$  ( $R_{vdW} = 65a_0$  and  $a_0$  is the Bohr radius). For  $r > \bar{a}$ , entrance- and closed-channel thresholds are set to be  $E = 0$  and  $E = \infty$ , respectively. Here  $\bar{a} = (\bar{V})^{1/3}$  and  $\bar{V} = \frac{1}{3\sqrt{2}} \frac{\Gamma(1/4)}{\Gamma(7/4)} R_{vdW}^3$  is the mean scattering volume [37], and  $\Gamma(x)$  is the gamma function. For the pair of  $^{40}\text{K}$  atoms we have the value  $\bar{a} = 63.4a_0$ .

Such a choice of the interatomic interaction permits a simple parametrization of the atom-atom scattering in universal terms of the energy of the bare bound state  $E_c$ , the Feshbach coupling strength  $\Gamma$  of the bound molecular state with the entrance channel and the background scattering volume  $V_{bg}$ , which is convenient for an analysis

of experimental data near magnetic Feshbach resonances [2, 33].

When the mixing between the closed channel and the entrance channel is weak and the background scattering length  $|a_{bg}|$  considerably exceeds the range of the interatomic interaction  $\bar{a}$ , the p-wave scattering volume  $V_p$  obeys the following expression

$$\frac{1}{V_p - \bar{V}} = \frac{1}{V_{bg} - \bar{V}} + \frac{\Gamma/2}{\bar{V}E_c} \quad (14)$$

The parameters  $V_{bg}$ ,  $\delta\mu$ ,  $B_0$ , and  $\Delta$  from [35] together with  $V_p(B)$  given by Eq.(5) are used for fitting the diagonal terms  $V_c$  and  $V_e$  in the tensor potential (13). The nondiagonal terms  $\hbar\Omega$  are defined by  $\Gamma/2 = 2\theta^2 V_c$ , where  $\tan 2\theta = 2\hbar\Omega/(V_e - V_c)$ .

The scattering volume  $V_p(B)$  is then calculated for different  $B$  and varying parameters of the potential  $\hat{V}$  by solving the Schrödinger equation

$$\left( \left[ -\frac{\hbar^2}{2\mu} \nabla^2 \right] \hat{I} + \hat{B} + \hat{V}(r) \right) |\psi\rangle = E|\psi\rangle \quad (15)$$

with scattering boundary condition

$$\psi_e(r) \rightarrow e^{ikz} + \frac{f(k, \theta)}{r} e^{ikr}, \psi_c(r) \rightarrow 0 \quad (16)$$

at  $kr \rightarrow \infty$  for the fixed  $E \rightarrow 0$  ( $k = \sqrt{2\mu E}/\hbar$ ) [38]. The diagonal matrix  $\hat{B}$  in Eq.(15) is defined as  $B_{cc} = \delta\mu(B - B_c)$  and  $B_{ee} = 0$ . After separation of the angular part in Eq.(15) we come to the system of two coupled radial equations

$$\left[ -\frac{\hbar^2}{2\mu} \frac{d^2}{dr^2} + \frac{\hbar^2 l(l+1)}{2\mu r^2} + B_{ii} \right] \phi_i(r) + \sum_j V_{ij}(r) \phi_j(r) = E \phi_i(r) \quad (17)$$

with  $l = 1$ , and  $i, j = e, c$ .

By setting  $\frac{C^{-2}(E)}{\tan \delta_{bg}(E)} = -\frac{V_{bg}\bar{V}}{(V_{bg}-V)^2}$  and varying  $V_c$ ,  $V_e$  and  $\Omega$  we obtain an excellent agreement of the calculated p-wave energy dependent scattering volume  $V_p(B, E) = -k^{-3} \tan \delta_1(B, k)$  (Eq.(1)) with the expression (5) from [35] for  $^{40}\text{K}$  atom in the hyperfine state  $|F = 9/2, m_F = -7/2\rangle$  for  $196G < B < 202G$ . The found zeros  $B^*$  and poles  $B_0$  of the scattering volume and the coupling strength  $\Gamma$  are given in Table I. Here  $B_c = B_0 + \beta\Delta$ ,  $\Delta = B^* - B_0$ , and  $\beta = V_{bg}/V_{bg} - \bar{V}$ . We note that such a procedure yields a  $k^3 \cot \delta_1(B, k)$  coinciding with the experimental data [34] for low colliding energies at  $T \sim 1-10nK$ . The agreement, however, weakens with increasing  $k$ . Therefore, our  $1/R = -1/2 \frac{d^2}{dk^2} (1/V_p(B, E))$  differs from the value given in [34] by about a factor of 3. This fact is, however, understandable because we did not use  $1/R$  directly from [34] in our fitting procedure for obtaining the parameters of the interaction potential (13).

Fig.1 shows our results obtained for the state  $m_l = 0$  for the scattering volume as a function of the magnetic

field  $B$  at the temperature  $T = 1.0nK$ . For comparison we have also plotted the analytical curve (5) which is in a good agreement with the numerical result. The computations were performed for  $V_e = 1.5 \times 10^{-2}[a.u.]$ ,  $V_c = 5.9 \times 10^{-2}[a.u.]$  and  $\Omega = 1.2 \times 10^{-6}[a.u.]$  modeling unbound two-atom states in the entrance channel  $|e\rangle$  and the resonance state with the parameters fixed for  $m_l = 0$  in the Table I.

### III. FESHBACH RESONANCE MODEL IN A WAVEGUIDE

Next we analyze the scattering properties of the p-wave magnetic Feshbach resonances in harmonic waveguides permitting unbound motion in the longitudinal  $z$ -direction and a transversally strongly confined  $\rho$ -motion in the potential  $1/2\mu\omega_\perp^2\rho^2$ . To describe the scattering process in the waveguide we have to calculate the scattering amplitude  $f_p(E)$  by integrating the Schrödinger equation

$$\left( \left[ -\frac{\hbar^2}{2\mu} \nabla^2 + \frac{1}{2}\mu\omega_\perp^2\rho^2 \right] \hat{I} + \hat{B} + \hat{V}(r) \right) |\psi\rangle = E|\psi\rangle \quad (18)$$

with the scattering boundary conditions

$$\psi_e(\mathbf{r}) = \left( \sin(k_0 z) + \text{sgn}(z) f_p e^{ik_0|z|} \right) \Phi_0(\rho), \quad \psi_{c,i}(\mathbf{r}) \rightarrow 0 \quad (19)$$

at  $|z| = |r \cos \theta| \rightarrow \infty$  adopted for a confining trap [13]. Here,  $\Phi_0(\rho)$  is the ground-state wave-function of the two-dimensional harmonic oscillator and  $k_0 = \sqrt{2\mu(E - \hbar\omega_\perp)}/\hbar = \sqrt{2\mu E_\parallel}/\hbar$ . We consider pair collisions of identical fermionic potassium atoms, therefore the scattering wave-function  $|\psi\rangle$  must be antisymmetric with respect to the exchange  $z \rightarrow -z$ . In the presence of the harmonic trap  $1/2\mu\omega_\perp^2\rho^2$  the azimuthal angular part of the solution is separated, and Eq.(18) is reduced to the coupled system of two 2D Schrödinger-type equations in the plane  $\{\rho, z\}$ . To integrate this coupled channel scattering problem in the plane  $\{r, \theta\}$  we have extended the computational scheme developed in [13]. The integration was performed in the units of the problem leading to the scale transformation:  $r \rightarrow \frac{r}{a}$ ,  $E \rightarrow \frac{E}{E_0}$ ,  $V \rightarrow \frac{V}{E_0}$ , and  $\omega_\perp \rightarrow \frac{\omega_\perp}{\omega_0}$  with  $E_0 = \frac{\hbar^2}{\mu a^2}$  ( $= 6.8 \times 10^{-9} E_h$  for  $^{40}\text{K}$  atoms), and  $\omega_0 = \frac{E_0}{\hbar}$  ( $= 2.8 \times 10^5 kHz$  for  $^{40}\text{K}$  atoms).

### IV. COMPUTATIONAL APPROACH

First, we discretize the Schrödinger Eq.(18) on a grid of the angular variable  $\{\theta_j\}_{j=1}^{N_\theta}$ , which has been introduced in [13]. We expand the solution of Eq.(18) in the basis  $g_j(\theta) = \sum_{l=0}^{N_\theta-1} P_l(\cos \theta) (\hat{P}^{-1})_{lj}$  according to

$$|\psi\rangle = \sum_{i=e,c} \psi_i(r, \theta) = \frac{1}{r} \sum_{i=e,c} \sum_{j=1}^{N_\theta} g_j(\theta) u_j^{(i)}(r), \quad (20)$$

where  $\hat{P}^{-1}$  is the inverse of the  $N_\theta \times N_\theta$  matrix  $\hat{P}$  with elements defined as  $P_{jl} = \lambda_j P_l(\cos \theta_j)$  and  $\lambda_j$  are the weights of the Gauss quadrature. Substituting (20) into (18) results in a system of  $2N_\theta$  Schrödinger-like coupled equations with respect to the  $2 \times N_\theta$  dimensional unknown vector  $\mathbf{u}(r) = \{u_{ji}(r)\} = \{\lambda_j^{1/2} u_j^{(i)}(r)\}_{j=1, i=e, c}^{N_\theta}$

$$[\hat{K}(x) + 2(E\hat{I} - \hat{U}(r(x)) - \hat{B})]\mathbf{u}(r(x)) = 0 \quad (21)$$

with

$$K_{jj'}^{ii'}(x) = [\delta_{jj'}\beta^2(x)(\frac{d^2}{dx^2} - \gamma\frac{d}{dx}) - \frac{1}{r^2} \sum_{l=0}^{N_\theta-1} P_{jl}l(l+1)(P^{-1})_{lj'}]\delta_{ii'} \quad (22)$$

and

$$U_{jj'}^{ii'}(r) = [V_{ii'}(r) + \frac{1}{2}\omega_\perp^2 \rho_j^2 \delta_{ii'}]\delta_{jj'}, \quad \rho_j = r \sin \theta_j. \quad (23)$$

with  $\beta(x) = (e^\gamma - 1)/(r_m \gamma e^{\gamma x})$  and we mapped and discretized the initial variable  $r \in (0, r_m]$  onto the uniform grid  $x_j \in (0, 1]$  according to

$$r_j = r_m \frac{e^{\gamma x_j} - 1}{e^\gamma - 1}, \quad j = 1, 2, \dots, N, \quad (24)$$

where  $r_m$  is chosen in the asymptotic region  $r_m \rightarrow \infty$  and  $\gamma > 0$  is a tuning parameter. Using the finite difference approximation, the above Schrodinger-like equations are reduced to a system of algebraic equations according to ref. [13]. By solving this system of equations for fixed colliding energy  $E$  and matching the calculated vector  $\psi_e(E, r = r_m, \theta_j)$  with the asymptotic behavior (19) at  $r = r_m$ , we find the scattering amplitude  $f_p$ , from which one can obtain the observable transmission coefficient  $T(E) = |1 + f_p(E)|^2$  in the waveguide.

## V. RESULTS AND DISCUSSION

### A. Transmission coefficient

We have performed two sets of integration of Eq.(18) for varying interatomic interaction (defined by a varying magnetic field  $B$ ) of  $^{40}\text{K}$  atoms in the hyperfine state  $|F = 9/2, m_F = -7/2\rangle$  and the relative angular momentum state  $|l = 1, m_l = 0\rangle$  near the Feshbach resonance  $B_0 = 198.85\text{G}$ : the dependence of the transmission  $T(B, \omega_\perp, \epsilon) = |1 + f_p(B, \omega_\perp, \epsilon)|^2$  on the trap frequency  $\omega_\perp$ , defining the transversal volume  $V_\perp = (\hbar/(\mu\omega_\perp))^{3/2}$ , and the rescaled longitudinal energy  $\epsilon = \frac{E_\parallel}{2\hbar\omega_\perp} = \frac{E - \hbar\omega_\perp}{2\hbar\omega_\perp} = \frac{E}{2\hbar\omega_\perp} - \frac{1}{2}$  was analyzed. Calculations were performed with the parameters  $V_e$ ,  $V_c$ , and  $\Omega$  of the interaction potential  $\hat{V}$  (13) fixed in Section II by fitting the parameters of the Feshbach resonance of potassium atoms in free space.

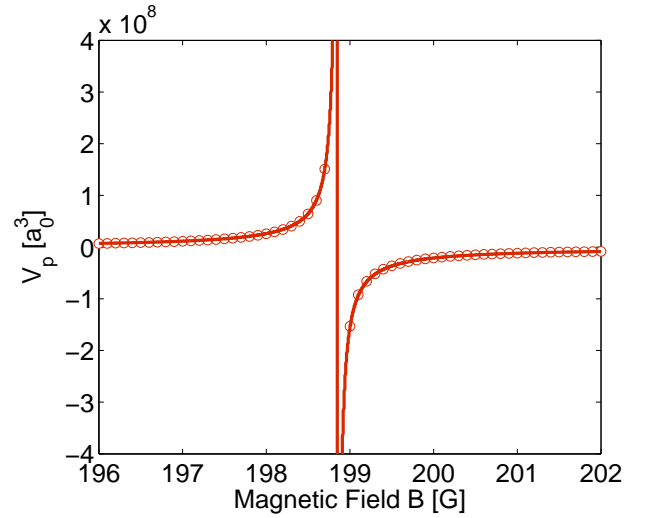


FIG. 1: (Color online) The p-wave scattering volume  $V_p$  calculated for potassium atoms near the Feshbach resonance in the hyperfine state  $|F = 9/2, m_F = -7/2\rangle$  and the relative angular momentum state  $|l = 1, m_l = 0\rangle$  as a function of the magnetic field  $B$ . The solid curve shows the analytical result (5) and the dots show the numerical result (see text).

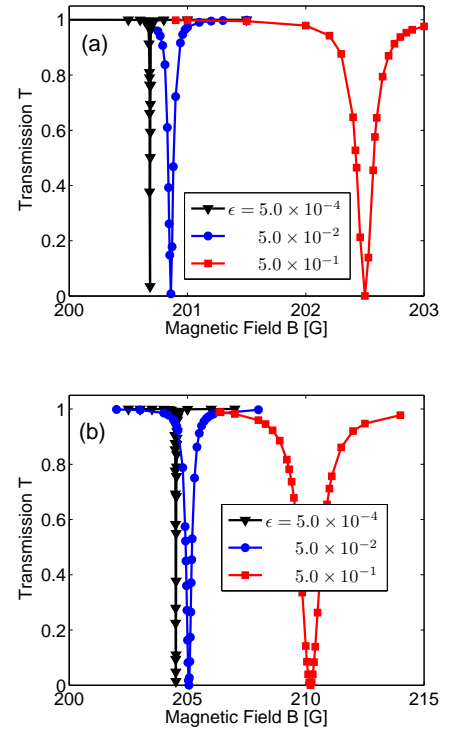


FIG. 2: (Color online) The transmission  $T$  in the harmonic waveguide with (a)  $\omega_\perp = 0.002$  and (b)  $\omega_\perp = 0.006$  as a function of external magnetic field  $B$  for several rescaled longitudinal energies  $\epsilon$ .

In Fig.2 the dependence of the transmission

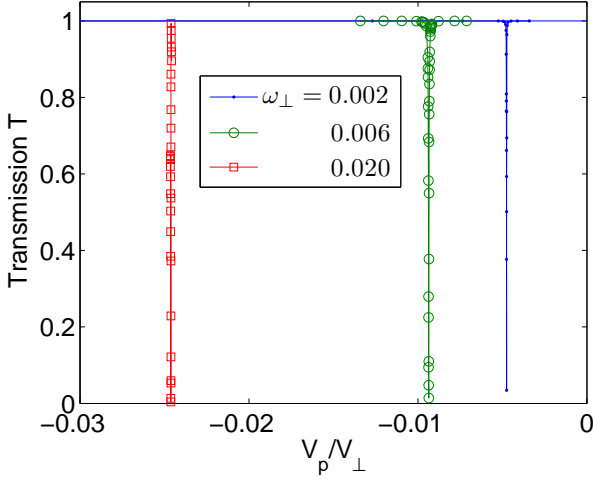


FIG. 3: (Color online) Transmission  $T$  in the waveguide for the low energy limit  $\epsilon = 5 \times 10^{-4}$  as a function of  $V_p/V_\perp$ .

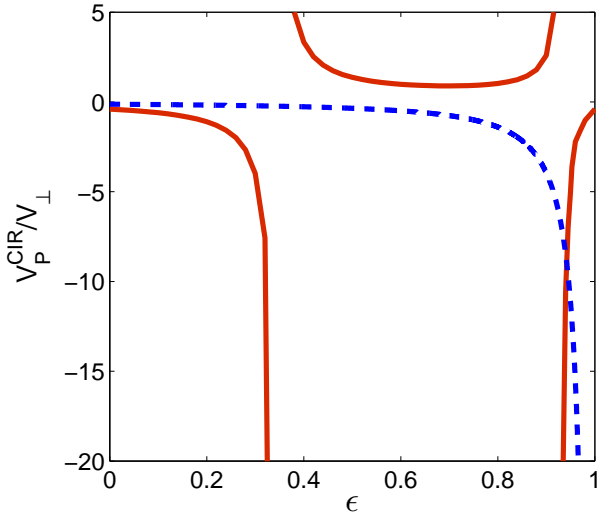


FIG. 4: (Color online) The position of the p-wave CIR in the harmonic waveguide as a function of  $\epsilon$  predicted by Eqs.(25) (solid curve) and (26) (dashed curve).

$T(B, \omega_\perp, \epsilon)$  on the external magnetic field  $B$  is given for two different  $\omega_\perp$  and varying colliding energy. The p-wave Feshbach resonance is manifested in the waveguide as a minimum in the transmission  $T(B_{CIR}) = 0$  (i.e. as a p-wave CIR)[13, 17, 23]. Fig.2 demonstrates the strong dependence of the shift of the resonance  $B_0 - B_{CIR}$  in the confining trap on the trap frequency  $\omega_\perp$  similar to the s-wave CIRs [32]. This effect, as in the case of the s-wave CIR [5, 6], can be used to control the p-wave CIR position. However, for a complete control of the p-wave resonance shift in the waveguide one has also to understand the strong dependence on the energy  $\epsilon$  shown in Fig.2. This effect has to be

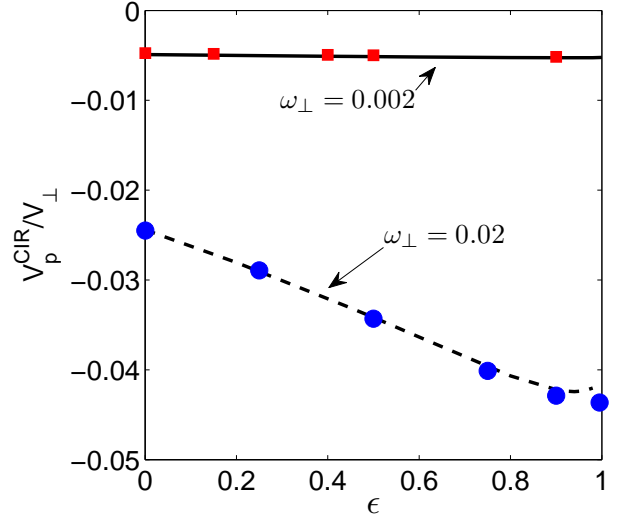


FIG. 5: (Color online) The position of the p-wave CIR as a function of  $\epsilon$  in harmonic waveguides with  $\omega_\perp = 0.002$  and  $0.02$ . The curves show the analytical results (29) and the dots correspond to the numerical results.

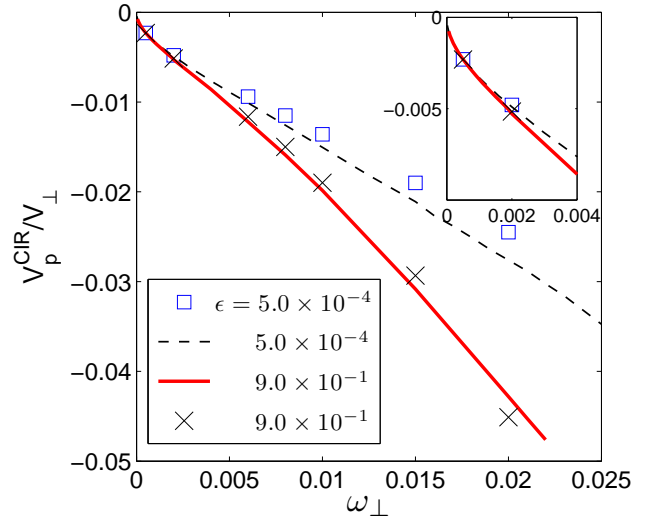


FIG. 6: (Color online) The position of the p-wave CIR in the harmonic waveguide as a function of  $\omega_\perp$ . The curves show the analytical results (29) and the dots correspond to the numerical results.

contrasted to the position of the s-wave CIR given by  $a_s(B_{CIR})/a_\perp = 0.68$  (where  $a_\perp = V_\perp^{1/3}$  and  $a_s$  is the s-wave scattering length) [1] which is taken in the  $\epsilon \rightarrow 0$  limit and was confirmed in recent experiments [5, 6]. The strong dependence of the p-wave CIR position on  $\epsilon$  is equally known [17]. However, subsequent investigations, both of analytical [19, 39] and numerical character [13], have demonstrated strong deviations from the results in ref. [17]. In the next subsection we shall discuss

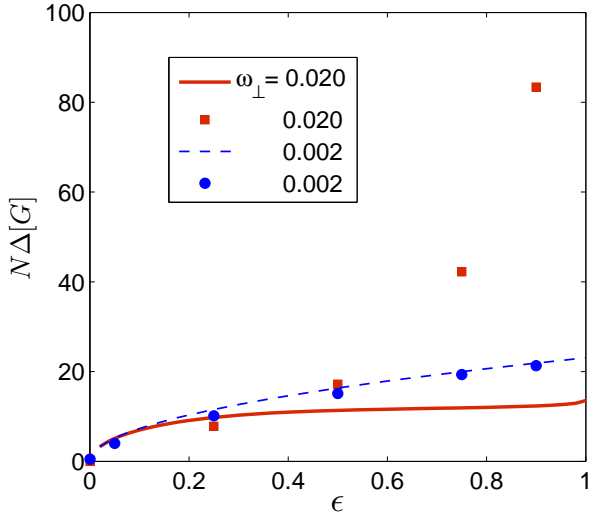


FIG. 7: (Color online) The width of the p-wave CIR of potassium atoms in the hyperfine state  $|F = 9/2, m_F = -7/2\rangle$  and the relative angular momentum state  $|l = 1, m_l = 0\rangle$  as a function of the rescaled energy  $\epsilon$  in harmonic waveguides with  $\omega_\perp = 0.002$  and  $0.02$ .  $N = 100$  and  $1$  for  $\omega_\perp = 0.002$  and  $0.02$  respectively. The curves show the analytical results (31) and the dots show the numerical results.

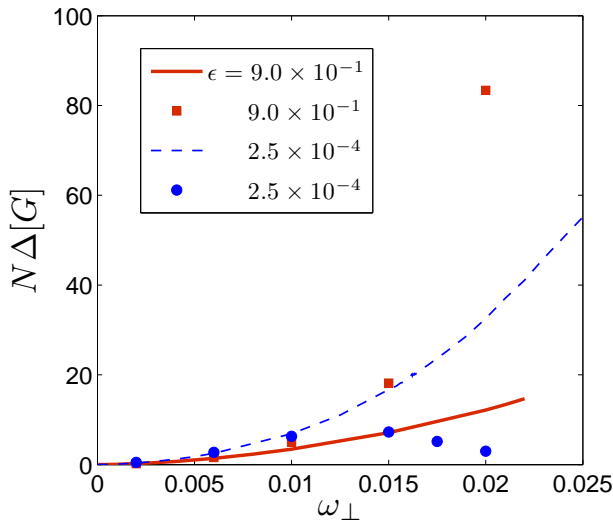


FIG. 8: ((Color online) The width of the p-wave CIR of potassium atoms confined by harmonic waveguide in the hyperfine state  $|F = 9/2, m_F = -7/2\rangle$  and the relative angular momentum state  $|l = 1, m_l = 0\rangle$  as a function of the waveguide frequency  $\omega_\perp$  for  $\epsilon = 5.0 \times 10^{-4}$  and  $9.0 \times 10^{-1}$ .  $N = 100$  and  $1$  for  $\epsilon = 5.0 \times 10^{-4}$  and  $9.0 \times 10^{-1}$  respectively. The curves show the analytical results (31) and the dots show the numerical results.

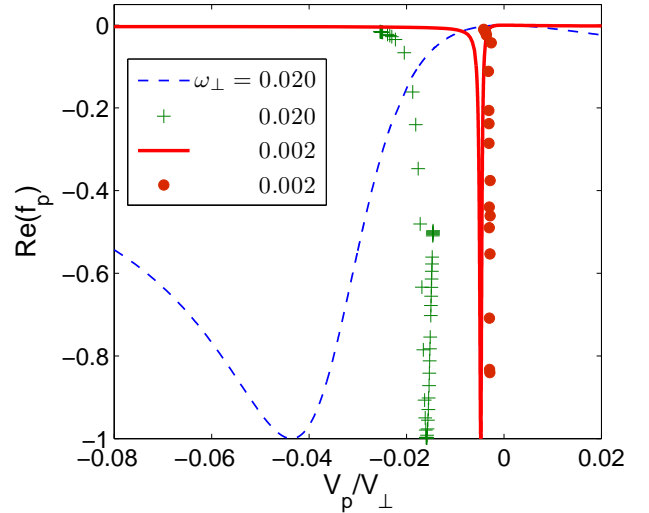


FIG. 9: (Color online) The real part of the scattering amplitude  $f_p$  (dots) as a function of the  $V_p/V_\perp$  along with the analytical results (30) (curves) for  $\epsilon = 0.9$ .

the origin of this difference. To this end we study the transmission  $T(V_p(B), \omega_\perp, \epsilon) = |1 + f_p(V_p(B), \omega_\perp, \epsilon)|^2$  as a function of the p-wave scattering volume  $V_p(B)/V_\perp$  “normalized” to the transversal volume  $V_\perp$  and as a function of the trap frequency  $\omega_\perp$  in the low energy limit, which is shown in Fig.3. The dependence of the p-wave CIR position  $V_p^{CIR}/V_\perp$ , defined as  $T(V_p^{CIR}/V_\perp) = 0$ , on  $\omega_\perp$  qualitatively shows the same behaviour as in our previous work [13]. However, the calculated values of  $|V_p^{CIR}/V_\perp|$  in [13] are approximately two times larger than the present values. This difference stems from the definition of  $V_p$  for the chosen interatomic interaction in [13]. Specifically, in [13] the effective range  $R$  was not included in the definition of the scattering volume  $V_p$  and the interatomic interaction was of single channel character, contrary to the tensorial structure of  $\hat{V}$  in (13). We note that we have shown recently [32] using a tensorial potential of type (13) that both these effects do not influence the position of the s-wave CIR.

### B. Shift of p-wave Feshbach resonance in harmonic waveguide

In [17] the CIR of a pair of identical fermions has been studied analytically by means of a fermion-boson mapping. In this way the authors have obtained the ratio

$$\frac{V_p^{CIR}}{V_\perp} = [12\zeta(-\frac{1}{2}, 1 - \epsilon)]^{-1} \quad (25)$$

for the position  $V_p^{CIR}$  of the CIR corresponding to the minimum in the transmission  $T$ . This ratio depends only on the rescaled longitudinal energy  $\epsilon$  and the dependence is defined by the Hurwitz zeta-function  $\zeta$ . In Fig.4 we

show the resonance position predicted by this formula as a function of  $\epsilon$  (the solid curve). On the other hand, in [19], the dependence of the p-wave CIR position on  $\epsilon$  is given by the simple expression

$$\frac{V_p^{CIR}}{V_\perp} = -[4(1 - \epsilon)]^{-3/2}, \quad (26)$$

predicting a smoother dependence on  $\epsilon$  and a strong deviation from (25) with varying  $\epsilon$  (see the dashed curve in Fig.4). Thus, both formulae exhibit a strong dependence of the p-wave CIR position on  $\epsilon$  in support of our above result (see Fig.2) but do not describe the strong dependence of the ratio  $V_p^{CIR}/V_\perp$  on the trap frequency  $\omega_\perp$  we find: see Fig.3 and Figs.10(a,b) in our previous work [13]. Our above analysis has shown that the origin of the drawback of both formulae (25) and (26) is the neglecting of the second term  $\frac{k^2}{R(B)}$  in Eq.(1) in the derivation of these formulae.

In a recent work [39] it was concluded that, unlike in the case of s-wave interaction, the p-wave effective range is essential in the strongly interacting regime i.e. near the corresponding Feshbach resonance and the shift of the p-wave magnetic Feshbach resonance in confining harmonic waveguide was calculated analytically. Assuming that the external magnetic field lies in the  $xz$ -plane with angle  $\phi$  with respect to the  $z$ -axis, and that the incoming particles are in the ground state of an axially symmetric harmonic confinement, the authors of [39] have obtained an analytical expression for the scattering wave function. They arrive at the energy dependent 1D scattering length:

$$a_{1D} = -\frac{\tan \delta_1}{k_0} = \frac{6a_\perp (D_{1x}^{1D} \cos^2 \phi + D_{0x}^{1D} \sin^2 \phi)}{\bar{D}_{0z}^{1D} D_{1x}^{1D} \cos^2 \phi + D_{0x}^{1D} \bar{D}_{1z}^{1D} \sin^2 \phi} \quad (27)$$

where  $k_0 = \sqrt{2\mu(E - \hbar\omega_\perp)}/\hbar = \frac{2\sqrt{\epsilon}}{a_\perp}$  ( $\epsilon = \frac{E}{2\hbar\omega_\perp} - \frac{1}{2}$ ),  $\bar{D}_{mz}^{1D} = D_m^{1D} - 12\zeta(-\frac{1}{2}, 1 - \epsilon)$ ,  $D_{mx}^{1D} = D_m^{1D} + C_x^{1D}(\epsilon)$ ,  $D_m^{1D} = \frac{V_\perp}{V_p} - \frac{2E}{\hbar\omega_\perp} \frac{a_\perp}{R}$  and  $C_x^{1D}(\epsilon)$  is a function defined in [39].

For anisotropic interaction ( $D_0^{1D} \neq D_1^{1D}$ ) with  $\phi = 0$  or  $\phi = \frac{\pi}{2}$  as well as for isotropic interaction ( $D_0^{1D} = D_1^{1D}$ ), one obtains:

$$a_{1D} = \frac{6a_\perp}{\bar{D}_{mz}^{1D}} \quad (28)$$

which yields a resonance ( $\bar{D}_{mz}^{1D} = 0$ ) at  $D_m^{1D} - 12\zeta(-\frac{1}{2}, 1 - \epsilon) = 0$ , from which one obtains for the resonance condition i.e. for the position of the p-wave CIR:

$$\frac{V_p^{CIR}(\epsilon)}{V_\perp} = \left[ \frac{2a_\perp}{R} + 12\zeta(-\frac{1}{2}, 1 - \epsilon) \right]^{-1}. \quad (29)$$

This formula is essentially different from Eqs.(25) and (26) by the presence of the term  $\frac{2a_\perp}{R} = \frac{2\sqrt{\hbar}}{R\sqrt{\mu\omega_\perp}}$ .

In our case of two spin-polarized  $^{40}\text{K}$  atoms  $|F = 9/2, m_F = -7/2\rangle$  with relative quantum numbers  $l = 1$

and  $m_l = 0$  trapped in the waveguide and equipped with a longitudinal magnetic field we expect the resonance position to obey Eq.(29). The results presented in Fig.5 demonstrate excellent agreement of our calculation of the p-wave CIR position  $V_p^{CIR}/V_\perp$  with the analytic result (29) in the complete region below the first threshold of transverse excitation  $\epsilon = 1$ , which persists in a broad range of varying  $\omega_\perp$ . Note also the emerging stronger than linear dependence on the energy  $\epsilon$  with increasing  $\omega_\perp$ .

Fig.6 shows the resonance position as a function of the trap frequency  $\omega_\perp$  for the zero energy limit  $\epsilon = 5 \times 10^{-4}$  as well as near the first threshold of transverse excitation  $\epsilon = 0.9$ . It demonstrates the close to linear dependence of the resonance position  $V_p^{CIR}/V_\perp$  on  $\sqrt{\omega_\perp}$  as  $\omega_\perp \rightarrow 0$  regardless of the value of the energy (see figure inside). The numerical results are in good agreement with Eq.(29).

### C. Width of p-wave Feshbach resonance

Next we analyze the widths of the p-wave CIRs in harmonic waveguides. Since at the resonant field  $B_{CIR}$  (corresponding to the position of CIR) the transmission reaches  $T(B_{CIR}) = 0$  and the maximal  $T$  value is 1 we define the width  $\Delta_{1D} = B_+ - B_-$ , where  $B_+$  and  $B_-$  are the fields correspondingly right and left to  $B_{CIR}$  and the transmission approaches the value  $T(B_\pm) = 1/2$ . This definition differs from that for a free space magnetic Feshbach resonance where it reads  $B^* - B_0$  [33]. By using the analytical formula for the scattering amplitude in ref. [40]

$$f_p(B) = \frac{-ik_0}{a_{1D}^{-1}(B) + Rk_0^2 + iK_0} \quad (30)$$

valid near the CIR in the zero-energy limit  $k_0 = \sqrt{2\mu E_\parallel}/\hbar = \sqrt{2\mu(E - \hbar\omega_\perp)}/\hbar \rightarrow 0$  and Eq.(28) we obtain

$$\Delta_{1D} = \Delta \left[ \frac{\alpha_+}{\alpha_+ - 1} - \frac{\alpha_-}{\alpha_- - 1} \right] \quad (31)$$

where  $\alpha_\pm = 6 \frac{V_{bg}}{a_\perp^2 a_{1D}(B_\pm)} + \frac{V_{bg}}{V_p^{CIR} R}$ . In Figs. 7 and 8 we show the calculated resonance width  $\Delta_{1D}$  as a function of the rescaled energy  $\epsilon$  and waveguide frequency  $\omega_\perp$ , respectively, together with the analytical result according to Eq.(31). One observes a good agreement for  $\omega_\perp < 0.01$ . However, we encounter major deviations with increasing  $\omega_\perp$  except for the zero energy limit  $\epsilon \rightarrow 0$ . These deviations are due to the fact that the analytical formula (30) which we used to derive (31), was obtained in the zero energy limit and does not work for larger energies. In Fig.9 we present the real part of our scattering amplitude  $\text{Re}(f_p)$  along with the analytical results from (30) as a function of  $V_p/V_\perp$  for  $\epsilon = 0.9$  (large energy) for comparison. As the trap frequency  $\omega_\perp$  increases we observe deviations between the analytical and numerical results for  $f_p$ .



The same way as in the case of the free space resonance, the width  $\Delta_{1D}$  of the CIR narrows with decreasing energy  $\epsilon$  (see Fig.7). Fig.8 shows that in a harmonic waveguide there is a region where we have a possibility for narrowing the width by decreasing the trap frequency.

## VI. CONCLUSION

We develop and analyze a theoretical model to study Feshbach resonances of identical fermions in atomic waveguides by extending the two-channel model suggested in [33] and adopted in [32] for confined bosons. In this model, the experimentally known parameters of Feshbach resonances in free space are used as an input. Within this approach we have calculated the shifts and widths of p-wave magnetic Feshbach resonance of  $^{40}\text{K}$  atoms in the hyperfine state  $|F = 9/2, m_F = -7/2\rangle$  and for the relative angular momentum state  $|l = 1, m_l = 0\rangle$  emerging in harmonic waveguides as p-wave CIRs. We find a linear dependence of the resonance position on the longitudinal colliding energy below the threshold for the first transverse excitation. It is shown that in a harmonic waveguide there is the possibility to decrease the width of the p-wave Feshbach resonance by decreasing

the (transversal) trap frequency which could be used in corresponding experiments. Our analysis demonstrates the importance of including the effective range terms in the computational schemes for the description of the p-wave CIRs contrary to the case of s-wave CIRs where the impact of the effective radius is negligible. In previous investigations of the p-wave CIRs in harmonic waveguides [13, 17, 23] the effects due to the effective range have been neglected. The developed model can be applied for a quantitative analysis of other p-wave CIRs following a different spin structure and for confining traps of different geometry including effects due to anharmonicity and anisotropy.

## VII. ACKNOWLEDGEMENTS

Sh.S would like to thank J. Abouie and S. Abedinpour for fruitful discussions. V.S.M. and P.S. acknowledge financial support by the Heisenberg-Landau Program. V.S.M. thanks the Zentrum für Optische Quantentechnologien of the University of Hamburg and Sh.S. thanks the Bogoliubov Laboratory of Theoretical Physics of JINR for their warm hospitality. This work was supported by IASBS (Grant No.G2014IASBS12648).

- 
- [1] M. Olshanii, Phys. Rev. Lett. **81**, 938 (1998).
  - [2] C. Chin, R. Grimm, P. Julienne, and E. Tiesinga, Rev. Mod. Phys. **82**, 1225 (2010).
  - [3] T. Kinoshita, T. Wenger, and D.S. Weiss, Science **305**, 1125 (2004).
  - [4] B. Paredes et al, Nature **429**, 277 (2004).
  - [5] E. Haller, M. Gustavsson, M.J. Mark, J.G. Danzl, R. Hart, G. Pupillo, and H.C. Nägerl, Science **325**, 1224 (2009).
  - [6] E. Haller, M.J. Mark, R. Hart, J.G. Danzl, L. Reichsöllner, V. Melezhik, P. Schmelcher, and H.C. Nägerl, Phys. Rev. Lett. **104**, 153203 (2010).
  - [7] H. Moritz, T. Stöferle, K. Guenter, M. Köhl, and T. Esslinger, Phys. Rev. Lett. **94**, 210401 (2005).
  - [8] K. Günter, T. Stöferle, H. Moritz, M. Köhl, and T. Esslinger, Phys. Rev. Lett. **95**, 230401 (2005).
  - [9] B. Fröhlich, M. Feld, E. Vogt, M. Koschorreck, W. Zwerger, and M. Köhl, Phys. Rev. Lett. **106**, 105301 (2011).
  - [10] G. Lamporesi, J. Catani, G. Barontini, Y. Nishida, M. Inguscio, and F. Minardi, Phys. Rev. Lett. **104**, 153202 (2010).
  - [11] T. Bergeman, M.G. Moore, and M. Olshanii, Phys. Rev. Lett. **91**, 163201 (2003).
  - [12] V.S. Melezhik, J.I. Kim, and P. Schmelcher, Phys. Rev. **A76**, 053611 (2007).
  - [13] S. Saeidian, V.S. Melezhik, and P. Schmelcher, Phys. Rev. **A77**, 042721 (2008).
  - [14] P. Giannakeas, V.S. Melezhik, and P. Schmelcher, Phys. Rev. **A84**, 023618 (2011).
  - [15] S. Sinha and L. Santos, Phys. Rev. Lett. **99**, 140406 (2007).
  - [16] P. Giannakeas, V.S. Melezhik, and P. Schmelcher, Phys. Rev. Lett. **111**, 183201 (2013).
  - [17] B.E. Granger and D. Blume, Phys. Rev. Lett. **92**, 133202 (2004).
  - [18] J.I. Kim, V.S. Melezhik, and P. Schmelcher, Phys. Rev. Lett. **97**, 193203 (2006).
  - [19] J.I. Kim, V.S. Melezhik, and P. Schmelcher, Progr. Theor. Phys. Supp. **166**, 159 (2007).
  - [20] V.S. Melezhik and P. Schmelcher, New J. Phys. **11**, 073031 (2009).
  - [21] V.S. Melezhik and P. Schmelcher, Phys. Rev. **A84**, 042712 (2011).
  - [22] M.G. Moore, T. Bergeman, and M. Olshanii, J. Phys. IV **116**, 69 (2004).
  - [23] J.I. Kim, J. Schmiedmayer, and P. Schmelcher, Phys. Rev. **A72**, 042711 (2005).
  - [24] P. Giannakeas, F.K. Diakonov, and P. Schmelcher, Phys. Rev. **A86**, 042703 (2012).
  - [25] E. Haller, M. Rabie, M.J. Mark, J.G. Danzl, R. Hart, K. Lauber, G. Pupillo, and H.C. Nägerl, Phys. Rev. Lett. **107**, 230404 (2011).
  - [26] S.G. Peng, S.S. Bohloul, X.J. Liu, H. Hu, and P.D. Drummond, Phys. Rev. **A82**, 063633 (2010).
  - [27] W. Zhang and P. Zhang, Phys. Rev. **A83**, 053615 (2011).
  - [28] S. Sala, P.-I. Schneider, and A. Saenz, Phys. Rev. Lett. **109**, 073201 (2012).
  - [29] E. Tiesinga, C.J. Williams, F.H. Mies, and P.S. Julienne, Phys. Rev. A **61**, 063416 (2000).
  - [30] V.A. Yurovsky, Phys. Rev. **A71**, 012709 (2005).
  - [31] S. Grishkevich, S. Sala, and A. Saenz, Phys. Rev. **A84**, 062710 (2011).
  - [32] S. Saeidian, V.S. Melezhik, and P. Schmelcher, Phys. Rev. **A86**, 062713 (2012).

- [33] A.D. Lange, K. Pilch, A. Prantner, F. Ferlino, B. Engeser, H.-C. Nägerl, R. Grimm, and C. Chin, Phys. Rev. **A79**, 013622 (2009).
- [34] C. Ticknor, C.A. Regal, D.S. Jin, and J.L. Bohn, Phys. Rev. A **69**, 042712 (2004).
- [35] Z. Idziaszek, Phys. Rev. A **79**, 062701 (2009).
- [36] P.S. Julienne and B. Gao (AIP, 2006), vol. 869, 261.
- [37] S. Gautam and D. Angom Eur. Phys. J. D **56**, 173 (2010).
- [38] V.S. Melezhik and C.-Y. Hu, Phys. Rev. Lett. **90**, 083202 (2003).
- [39] Shi-Guo Peng, S. Tan, and K. Jiang, arXiv:1312.3392v2.
- [40] Tao Shi and Su Yi, Phys. Rev. A **90**, 042710 (2014).